Am J Cancer Res 2011;1(1):1-13
www.ajcr.us /ISSN:2156-6976/ajcr0000003

Original Article

Genomic profiling of genes contributing to metastasis in a mouse model of thyroid follicular carcinoma

Changxue Lu[1], Alok Mishra[1], Yuelin J Zhu[2], Paul Meltzer[2], Sheue-yann Cheng[1]

[1]*Laboratory of Molecular Biology, and* [2]*Laboratory of Cancer Genetics, Center for Cancer Research, National Cancer Institute, Bethesda, MD 20892, USA.*

Received September 21, 2010; accepted September 29, 2010; Epub September 30, 2010; Published January 1, 2011

Abstract: Metastasis is the major cause of thyroid cancer-related death. However, little is known about the genes involved in the metastatic spread of thyroid carcinomas. We have created a mouse that spontaneously develops metastatic follicular thyroid carcinoma (FTC). This mouse harbors a targeted mutation (denoted TRβPV) in the thyroid hormone receptor β gene (*Thrb*$^{PV/PV}$ mice). Our recent studies show that the highly elevated level of thyroid stimulating hormone (TSH) in *Thrb*$^{PV/PV}$ mice promotes proliferation of thyroid tumor cells, but requires the collaboration of the oncogenic action of TRβPV to empower the tumor cells to undergo distant metastasis. To uncover genes destined to drive the metastatic process, we used cDNA microarrays to compare the genomic expression profile of laser capture microdissected thyroid tumor lesions of *Thrb*$^{PV/PV}$ mice with that of hyperplastic thyroid cells of wild-type mice having elevated TSH induced by treatment with the anti-thyroid drug propylthiouracil (WT-PTU mice). Analyses of microarray data indicated that the expressions of 150 genes were significantly altered between *Thrb*$^{PV/PV}$ and WT-PTU mice (87 genes had higher expression and 63 genes had lower expression in *Thrb*$^{PV/PV}$ mice than in WT-PTU mice). Thirty-six percent of genes with altered expression function as key regulators in metastasis. The remaining genes were involved in various cellular processes including metabolism, intracellular trafficking, transcriptional regulation, post-transcriptional modification, and cell-cell/extracellular matrix signaling. The present studies have uncovered novel genes responsible for the metastatic spread of FTC and, furthermore, have shown that the metastatic process of thyroid cancer requires effective collaboration among genes with diverse cellular functions. Importantly, the present studies indicate that the tumor cells in the primary lesions are endowed with the genes destined to promote metastasis. Thus, our study has provided new insights into the understanding of the metastatic spread of human thyroid cancer.

Keywords: Metastasis, thyroid cancer, mouse model, microarray, gene expression

Introduction

Thyroid cancers constitute the most frequent endocrine neoplasia, and their incidence has risen over the past several decades. Thyroid cancers in humans consist of an array of different histologic and biological types (papillary, follicular, medullary, clear cell, anaplastic, Hurthle cell, and others) [1], but the majority of clinically important human thyroid cancers are of the papillary and follicular types. Papillary thyroid carcinomas commonly metastasize to lymph nodes and are often multifocal, whereas follicular carcinomas show blood-borne metastases. While overall survival of patients with these types of tumor is generally better than for many other cancers, approximately 30% of patients do not survive beyond 20 years, even with successful primary surgical therapy. Recurrence of the tumor with metastasis becomes the major cause for thyroid cancer-related death. The genetic basis for this invasive or metastatic behavior is poorly understood. Animal models exhibiting metastatic spread would be useful in elucidating the molecular basis of metastatic thyroid cancer.

Accordingly, we have generated a mouse model (*Thrb*$^{PV/PV}$ mice) that spontaneously develops metastatic follicular thyroid cancer (FTC). This mouse harbors a knockin dominant negative mutation, known as PV, in the *Thrb* gene locus

[2]. The PV mutation was identified in a patient suffering from resistance to thyroid hormone (RTH) [3]. PV has a frame-shift mutation in the carboxyl-terminal 14 amino acids, resulting in a complete loss of thyroid hormone (T3) binding activity and transcriptional capacity [3]. Similar to an RTH patient who had two mutated *THRB* genes [4], *Thrb*$^{PV/PV}$ mice exhibit highly elevated serum thyroid stimulating hormone (TSH) [2, 5]. Remarkably, as *Thrb*$^{PV/PV}$ mice age, their thyroids undergo pathological changes from hyperplasia to capsular and vascular invasion, anaplasia, and eventual metastasis to the lung and sometimes to the heart [5]. The pathological progression, route, and frequency of metastasis in *Thrb*$^{PV/PV}$ mice are similar to that in human FTC.

Extensive molecular analyses of altered signaling pathways during thyroid carcinogenesis further validated that the *Thrb*$^{PV/PV}$ mouse is a preclinical mouse model of FTC. As found in human FTC, *Thrb*$^{PV/PV}$ mice exhibit similar aberrant signaling pathways that include constitutive activation of phosphatidyl inositol 3-kinase (PI3K)/Akt [6, 7], repression of peroxisome proliferator-activated receptor γ signaling [8, 9], and aberrant accumulation of both the pituitary tumor transforming gene (PTTG) [10, 11] and β-catenin [12]. Thus, the *Thrb*$^{PV/PV}$ mouse model faithfully recapitulates the molecular aberrations found in human thyroid cancer and is suitable for further identification by genomic profiling of genes that contribute to metastasis.

We have recently shown TSH is required for thyrocyte proliferation, but not sufficient for metastatic thyroid carcinogenesis of *Thrb*$^{PV/PV}$ mice [13]. This finding has facilitated the search for metastatic genes during thyroid carcinogenesis of *Thrb*$^{PV/PV}$ mice. In the present study, we compared the genomic expression profiles of laser capture microdissected thyroid lesions of *Thrb*$^{PV/PV}$ mice that have highly elevated TSH levels with that of hyperplastic follicular cells of wild-type mice that also have highly elevated TSH induced by propylthiouracil treatment (WT-PTU). By doing so, the identification of genes responsible for metastatic process was therefore simplified, as the expression of genes induced by TSH would not be considered. Indeed, we found distinctly different genomic expression profiles between thyroid cancer cells of *Thrb*$^{PV/PV}$ mice and hyperplastic follicular cells of WT-PTU mice. Among the 19 metastatic genes identified, 18 novel metastatic genes were uncovered in thyroid tumor cells. The identification of these novel genes suggests that the tumor cells in the primary lesions are endowed with the genes destined to promote metastasis. Furthermore, in addition to altered expression of genes acting in the metastatic process, we have also found altered expression of genes involved in various cellular processes including metabolism, intracellular trafficking, transcriptional regulation, post-transcriptional modification, and cell-cell/extracellular matrix (ECM) signaling. These results show that the metastatic process requires the collaboration of metastatic genes with diverse cellular signaling pathways for tumor cells to invade and to migrate to distant target sites.

Materials and methods

Animals

The animal protocols used in the study were approved by the NCI Animal Care and Use Committee. Mice harboring the TRβPV gene (*Thrb*$^{PV/PV}$ mice) were generated as previously described [2]. To generate mice with a high TSH level, wild-type (WT) siblings of *Thrb*$^{PV/PV}$ mice were fed with an iodine-deficient diet supplemented with 0.15% propylthiouracil (PTU) (Harlan Teklab) ad libitum starting at the age of 2 months. Thyroid tissues were collected from mice when they reached 10 months old and stored at -80°C for further analyses.

Laser capture microdissection, RNA extraction and amplification

Laser capture microdissection (LCM) was performed on the thyroid sections that were verified by histopathological analysis. Briefly, sections (5- to 8-μm) were cut from the OCT (optimal cutting temperature) compound blocks (cat. no. 4583, Tissue Tek, Sakura Finetek USA, Inc.) on PEN (polyethylene naphthalate) membrane slides (cat no. LCM 0522, MDS Analytical Technologies). LCM was then performed using an Arcturus^{XT} (Arcturus Engineering, Inc.) or a Veritas (Arcturus Engineering, Inc) machine. Captured cells attached to the polymer film surface on the CapSure Macro LCM caps (Arcturus Engineering, Inc.) were used for RNA extraction with PicoPure kit (cat. no. KIT#0202, Arcturus Biosciences, Inc.) according to the manufacturer's instructions.

The extracted total RNA was amplified with the use of a MessageAmp^{TM}II aRNA amplification kit

(AM 1751, Ambion) following the kit's protocol. In short, RNA (0.1-1.0 ng) was subjected to two rounds of amplification, and enriched aRNA was labeled with biotin-11-UTP for microarray hybridization. The quantity, integrity, and quality of biotinylated aRNA were assessed by Nanodrop (Thermo Scientific) and 2100 Bioanalyzers (Agilent Technologies). Mouse *Pax8* gene was used as a positive control to validate the thyroid tissue specificity by RT-PCR. The primers for murine *Pax8* were FP: 5'-CAC CTT CGT ACG GAC ACC TT-3' and RP: 5'-GTT GCG TCC CAG AGG TGT AT- 3'.

Microarray analysis

Biotinylated-aRNA samples from three individual mice of each group were used in hybridization of the GeneChip Mouse Genome 430 2.0 array (Affymetrix, Santa Clara, CA) and scanned on an Affymetrix GeneChip scanner 3000. Data were collected using Affymetrix GCOS software. Statistical and clustering analyses were performed with Partek Genomics Suite software using the robust multichip average (RMA) normalization algorithm. Differentially expressed genes were identified with ANOVA analysis. Genes that were up- or down-regulated more than 1.5 fold and with a p <0.05 were considered significant. Significant genes were analyzed for enrichment of pathways and functions using the DAVID bioinformatics database (http://david.abcc.ncifcrf.gov/) [14, 15] and Ingenuity Pathway Analysis (IPA, Ingenuity Systems, Inc., Redwood City, CA).

Real time RT-PCR validation of microarray data

Selected genes from microarray data were chosen for real time RT-PCR validation. A total 50 ng of RNA extracted from thyroids of $Thrb^{PV/PV}$ or WT-PTU mice was used in the real-time RT-PCR. The reactions were performed with the QuantiTech SYBR RT-PCR kit (Qiagen, Germantown, MD) on an ABI 7900HT system. In each group, four to six samples with triplicates were tested on the target genes. Data were analyzed using Prism V5 (GraphPad Software, Inc., La Jolla, CA). Primers used in RT-PCR are listed in Supplementary Table 1.

Results

Analysis of gene expression profiles of hyperplastic follicular cells of WT-PTU mice and thyroid tumor cells of $Thrb^{PV/PV}$ mice

Array data were obtained from laser capture microdissected thyroid samples of age-matched male wild-type (WT) mice, WT-PTU mice, and $Thrb^{PV/PV}$ mice (n=3 for each type of mice). **Figure 1A** shows the results of principal component analysis (PCA) of the gene expression profiles from WT mice with normal TSH levels, WT-PTU mice with highly elevated TSH levels, and $Thrb^{PV/PV}$ mice with highly elevated TSH levels. The three-dimensional projection of the top three principal components of PCA, capturing 66.7% of total variance, shows clear separation of the three groups (**Figure 1A**). The well-segregated three clusters of data derived from WT, WT-PTU, and $Thrb^{PV/PV}$ mice, respectively, allowed us to compare the changes in gene expression due to TSH (compare WT with WT-PTU mice) or due to combined effects of TSH and TRβPV (compare WT with $Thrb^{PV/PV}$ mice). Subsequent comparison of gene expression profiles between the TSH-mediated effect and the effects due to combined actions of TSH and TRβPV allowed us to sort out the gene expression profiles due to the oncogenic actions of TRβPV critical for metastasis. Comparison of the array data between $Thrb^{PV/PV}$ and WT-PTU mice showed that 150 genes (Supplementary Table 2) exhibited altered expression (>1.5-fold change, p <0.05). In $Thrb^{PV/PV}$ mice, 87 genes were up-regulated and 63 genes were down-regulated. Among the up- and down-regulated genes, 13 (14.9%) and 8 (16%), respectively, were unnamed genes. A heat map displays the top 50 differentially expressed genes in the thyroid tumor cells of $Thrb^{PV/PV}$ mice by hierarchical clustering (**Figure 1B**). It is clear that the gene expression profiles mediated by TSH alone in WT-PTU were strikingly distinct from those mediated by the combined actions of TSH and TRβPV in $Thrb^{PV/PV}$ mice.

Functional classification of genes with altered expression in thyroid tumor cells of $Thrb^{PV/PV}$ mice

The gene ontology analyses were first performed by using both the Gene Ontology Consortium tool available at http://www.informatics.jax.org and the Database for Annotation, Visualization and Integrated Discovery (DAVID) v6.7 (http://david.abcc.ncifcrf.gov/) [14, 15]. These two approaches provided a comprehensive analysis of molecular functions

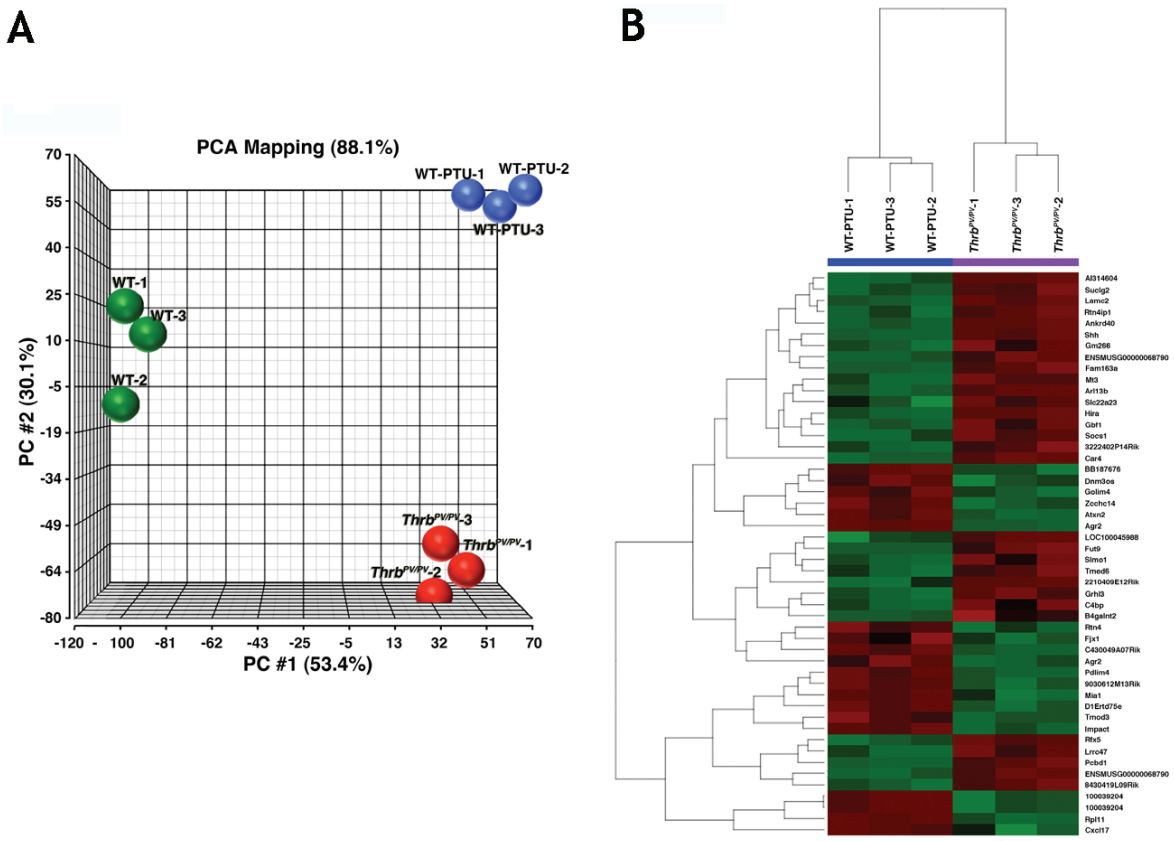

Figure 1. Principal component analysis (PCA) of the gene expression profiles in *Thrb*$^{PV/PV}$, WT-PTU, and WT mice (A), and a heat-map of hierarchical clustering in the top 50 genes with altered expression between *Thrb*$^{PV/PV}$ mice and WT-PTU mice (B). A. Three-dimensional projection of the top three principal components of PCA in the figure, which captures 66.7% of total variance, shows clear separation of the three groups. B. A heat-map presentation of hierarchical clustering (average of Euclidean distance) analysis of the top 50 genes filtered by the adjusted *p* values as described [38] and minimum 1.5-fold change in the comparison of *Thrb*$^{PV/PV}$ mice and WT-PTU mice.

and classification of each named gene. The functional classification analyzed by DAVID is presented in Supplementary Table 3. This table shows that 24.7% (37/150 total genes) were related to cell development and differentiation during embryogenesis. Twenty-four percent of genes (36/150) were found in the category with functions related to maintaining cell structure, cell movement, or cell-to-cell signaling. About 9% of the identified genes regulated immune response, and approximately 10% regulated metabolism.

In addition, we also searched the PubMed database for each named gene in combination with the following terms: tumor, metastasis, thyroid, thyroid tumor, invasion, mobility, immune response, and stem cells. Combined with results of DAVID and IPA analyses, the altered genes between *Thrb*$^{PV/PV}$ and WT-PTU were grouped in three major categories (**Table 1**: Metastasis/invasion-related genes; **Table 2**: Tumor-related genes; **Table 3**: Genes with other cellular functions), signifying molecules with wide diverse functions and complex signaling pathways during metastatic thyroid carcinogenesis of *Thrb*$^{PV/PV}$ mice.

Since it is not possible to detail the cellular functions for each of 150 genes that had altered expression within the journal space allowed, only the genes that were well-studied in other cancers are highlighted in each category as shown below. Readers should refer to the

Table 1. Metastasis-related genes (n=19) with altered expression in thyroid tumors of *Thrb*$^{PV/PV}$ mice

Gene symbol	Gene name	Fold change (microarray/RT-PCR)
Olfm4*	olfactomedin 4	5.52/4.14
Muc4*	mucin 4, cell surface associated	3.85/2.02
Cldn6	claudin 6	3.22
Grhl3	grainyhead-like 3 (Drosophila)	2.53//1.76
Ddr1	discoidin domain receptor tyrosine kinase 1	2.5/1.32
Emp2*	epithelial membrane protein 2	2.43/1.38
Lamc2	laminin, gamma 2	2.26
Atrn	attractin	2.18
Hmga1	high mobility group AT-hook 1	1.83
Il11*	interleukin 11	1.64/1.60
Il13ra2*	interleukin 13 receptor, alpha 2	0.53/0.57
Agr2	anterior gradient homolog 2 (Xenopus laevis)	0.51/0.60
Rock1	Rho-associated, coiled-coil containing protein kinase 1	0.5
Sec14l2	SEC14-like 2 (S. cerevisiae)	0.43
Afp	alpha-fetoprotein	0.36
Pdlim4	PDZ and LIM domain 4	0.33
Mia	melanoma inhibitory activity	0.33
Nr2f2	nuclear receptor subfamily 2, group F, member 2	0.3/0.43
Cxcl17	chemokine (C-X-C motif) ligand 17	0.23/0.24

* Genes discussed in the text.

Supplemental Tables 2 and 3 for the genes that they are interested in.

Uncovering of novel metastasis-related genes in thyroid tumor cells of Thrb$^{PV/PV}$ mice

Table 1 lists 19 genes that contribute to tumor metastasis in the microdissected thyroid lesions of *Thrb*$^{PV/PV}$ mice. The gene names and symbols are listed for easy reference. These genes account for 14.4% of the total named genes involved in cell-cell interaction, ECM interaction and signaling, cell migration, and angiogenesis. All these functions are critical for cell migration and invasion. Among these genes, 10 were up-regulated (52.6%), ranging from 1.64- to 5.52-fold; the other 9 genes were down-regulated, ranging from 1.87- to 4.35-fold. These genes are reported to play a role in cell invasion and metastasis in other cancers. However, except for the *Nr2f2* gene that was studied as a potential marker for diagnosis of thyroid cancer [16], all other 18 genes listed in **Table 1** were uncovered in the present study to play a role in migration and invasion of thyroid tumor cells of *Thrb*$^{PV/PV}$ mice.

At the top of the list (**Table 1**) is the extracellular matrix glycoprotein olfactomedin 4 (*Olfm4*) gene. The Olfm4 mRNA level was 5.52-fold higher in thyroid tumors of *Thrb*$^{PV/PV}$ mice shown by array analysis, and the increase was further shown by real time RT-PCR analysis (4.14-fold; **Figure 2A**). Over-expression of Olfm4 has been found in gastric cancer, pancreatic cancer, and colorectal carcinomas [17-19] and serves as an early diagnostic marker for gastric cancer patients [19]. The gene with the second highest activation was the mucin 4 gene (*Muc4;* 3.85-fold increase by array analysis). Its increased expression was also shown by real time RT-PCR analysis (**Figure 2B**). Overexpressed Muc4 has been observed in various preneoplastic and neoplastic lesions [20, 21]. In addition to its role in cell adhesion, this membrane protein has also been implicated in the regulation of cellular growth signaling through its interaction with the ErbB family of growth factor receptor tyrosine kinases (RTKs).

The epithelial membrane protein gene 2 (*Emp2*) also caught our attention (**Table 1**) (2.4-fold activation by array analysis and 1.38-fold by real time RT-PCR determination; **Figure 2C**). This gene encodes a tetraspan protein Emp2, a key regulator in cell adhesion and invasion. Emp2 also plays a role in trafficking proteins such as integrin αvβ3 and other key membrane recep-

Table 2. Tumor-related genes (n=35) with altered expression in thyroid tumors of *Thrb*$^{PV/PV}$ mice

Gene symbol	Gene name	Fold change (microarray/RT-PCR)
Fgg*	fibrinogen gamma chain	10.9/5.23
Slc39a4	solute carrier family 39 (zinc transporter), member 4	9.09/3.60
Slc5a5	solute carrier family 5	5.98
Shh*	sonic hedgehog homolog (Drosophila)	5.8/2.94
Esrrb*	estrogen-related receptor beta	4.00/2.94
B4galnt2	beta-1,4-N-acetyl-galactosaminyl transferase 2	3.55
Lad1	ladinin 1	3.35/3.206
Kdm6b	lysine (K)-specific demethylase 6B	2.88
Tceal1	transcription elongation factor A (SII)-like 1	2.65
Mapk6	mitogen-activated protein kinase 6	2.59
Thy1	Thy-1 cell surface antigen	2.57
Rfx4	regulatory factor X, 4	2.25/31.4
Mt3	metallothionein 3	2.21
Grhl2	grainyhead-like 2 (Drosophila)	2.1/1.41
Psd3	pleckstrin and Sec7 domain containing 3	2.09
Rfx5	regulatory factor X, 5	2.08
Hnf1b*	HNF1 homeobox B	1.95/6.03
Gfra1	GDNF family receptor alpha 1	1.9
Rrn3	RRN3 RNA polymerase I transcription factor homolog (S. cerevisiae)	1.82
Idh2	isocitrate dehydrogenase 2 (NADP+), mitochondrial	1.81
Cyb5b	cytochrome b5 type B (outer mitochondrial membrane)	1.7
Egln3	egl nine homolog 3 (C. elegans)	1.65
Hspa4l	heat shock 70kDa protein 4-like	1.53
Krt8	keratin 8	0.67
Sra1	steroid receptor RNA activator 1	0.58
Elf2	E74-like factor 2 (ets domain transcription factor)	0.52
Alcam	activated leukocyte cell adhesion molecule	0.44
Sptbn1	spectrin, beta, non-erythrocytic 1	0.44
Lman1	lectin, mannose-binding, 1	0.43
Fstl1	follistatin-like 1	0.4
Tmod3	tropomodulin 3 (ubiquitous)	0.35
Slc12a2	solute carrier family 12 (sodium/potassium/chloride transporters), member 2	0.33
Atxn2	ataxin 2	0.29
Map3k2	mitogen-activated protein kinase kinase kinase 2	0.19
Prdm6	PR domain containing 6	0.1

* Genes discussed in the text.

tors for efficient signaling transduction by membrane receptors [22].

Tumor-related immune response signaling in the microenvironment of thyroid tumor cells could promote metastasis. Mediators of tumor-related immune response may provide the favorable microenvironment for the growth of tumor cells. **Table 1** shows the altered expression of interleukin (*Il11,* also see **Figure 2D**) and down-regulation of interleukin 13 receptor, α2 (*Il13ra2*; also see **Figure 2E**). Interleukin-11 is a pleiotropic cytokine that was reported to be over-expressed in endometrial [23] and colorectal adenocarcinoma [24]. In colorectal adenocarcinoma, IL-11 promotes the tumor cell invasion via PI3K signaling and the p42/p44 MAPK pathway [24]. Consistent with these findings, we have recently reported the increased PI3K-AKT and p38 MAPK signaling during thyroid carcinogenesis of *Thrb*$^{PV/PV}$ mice [6, 13]. The *Il13ra2* gene encodes Il13 receptor α2 (Il13Rα2), a subunit of the interleukin 13 receptor complex. In human pancreatic cancer cells and glioblastoma, Il13Rα2 has been considered as a tumor antigen with therapeutic potential [25, 26]. In thyroid tumor cells of *Thrb*$^{PV/PV}$ mice, the suppression in the expression of *Il13ra2* gene could imply weakened immunosuppression that could favor metastatic potential of tumor cells.

The validation of these genes relevant in cell

Table 3. Genes with diverse cellular functions (n=56) that have altered expression in thyroid tumors of *Thrb*$^{PV/PV}$ mice

Gene symbol	Gene name	Fold change
Ca4*	carbonic anhydrase IV	6.69
Got1*	glutamic-oxaloacetic transaminase 1, soluble (aspartate aminotransferase 1)	5.78
Ppp2r3a	protein phosphatase 2 (formerly 2A), regulatory subunit B, alpha	4.64
Sbf1	SET binding factor 1	4.39
Slc22a23	solute carrier family 22, member 23	3.28
Fxyd4	FXYD domain containing ion transport regulator 4	3.11
Kif5c*	kinesin family member 5C	2.94
Rbm20	RNA binding motif protein 20	2.91
Pcbd1*	pterin-4 alpha-carbinolamine dehydratase/dimerization cofactor of hepatocyte nuclear factor 1 alpha	2.86
Dusp14	dual specificity phosphatase 14	2.79
Suclg2	succinate-CoA ligase, GDP-forming, beta subunit	2.78
Mtm1	myotubularin 1	2.73
B3gnt1	UDP-GlcNAc:betaGal beta-1,3-N-acetylglucosaminyltransferase 1	2.65
Trpm3	transient receptor potential cation channel, subfamily M, member 3	2.53
Rcor1	REST corepressor 1	2.49
Socs1*	suppressor of cytokine signaling 1	2.47
Lsm2	LSM2 homolog, U6 small nuclear RNA associated (S. cerevisiae)	2.47
Dync1i1*	dynein, cytoplasmic 1, intermediate chain 1	2.35
Fut9	fucosyltransferase 9 (alpha (1,3) fucosyltransferase)	2.32
Rtn4ip1	reticulon 4 interacting protein 1	2.30
Rnasek	ribonuclease, RNase K	2.09
Lonp1	lon peptidase 1, mitochondrial	2.08
Map6d1	MAP6 domain containing 1	1.95
Hira	HIR histone cell cycle regulation defective homolog A (S. cerevisiae)	1.94
Ppif	peptidylprolyl isomerase F	1.88
Arl13b	ADP-ribosylation factor-like 13B	1.86
Med20	mediator complex subunit 20	1.76
Flrt1	fibronectin leucine rich transmembrane protein 1	1.64
Usp3*	ubiquitin specific peptidase 3	1.56
Dph2	DPH2 homolog (S. cerevisiae)	1.51
Gbf1*	golgi-specific brefeldin A resistant guanine nucleotide exchange factor 1	1.51
Otud7a*	OTU domain containing 7A	0.65
Rnf130	ring finger protein 130	0.64
Sp3*	Sp3 transcription factor	0.60
Rpl11	ribosomal protein L11	0.59
N6amt2	N-6 adenine-specific DNA methyltransferase 2 (putative)	0.58
Gfod1	glucose-fructose oxidoreductase domain containing 1	0.58
Foxn3	forkhead box N3	0.57
Mbd5	methyl-CpG binding domain protein 5	0.57
Pnliprp2	pancreatic lipase-related protein 2	0.56
Tacr3	tachykinin receptor 3	0.54
Trove2	TROVE domain family, member 2	0.50
Oxtr	oxytocin receptor	0.48
Tgs1	trimethylguanosine synthase homolog (S. cerevisiae)	0.47
Usp37*	ubiquitin specific peptidase 37	0.46
Tbc1d20*	TBC1 domain family, member 20	0.45
Rpl37	ribosomal protein L37	0.45
Fjx1	four jointed box 1 (Drosophila)	0.44
Golim4*	golgi integral membrane protein 4	0.41
Olfm1	olfactomedin 1	0.37
Taok1	TAO kinase 1	0.35
Cldnd1	claudin domain containing 1	0.35
Ggps1	geranylgeranyl diphosphate synthase 1	0.31
Rc3h2	ring finger and CCCH-type zinc finger domains 2	0.30
Tor1b	torsin family 1, member B (torsin B)	0.28
Zranb1*	zinc finger, RAN-binding domain containing 1	0.21

* Genes discussed in the text.

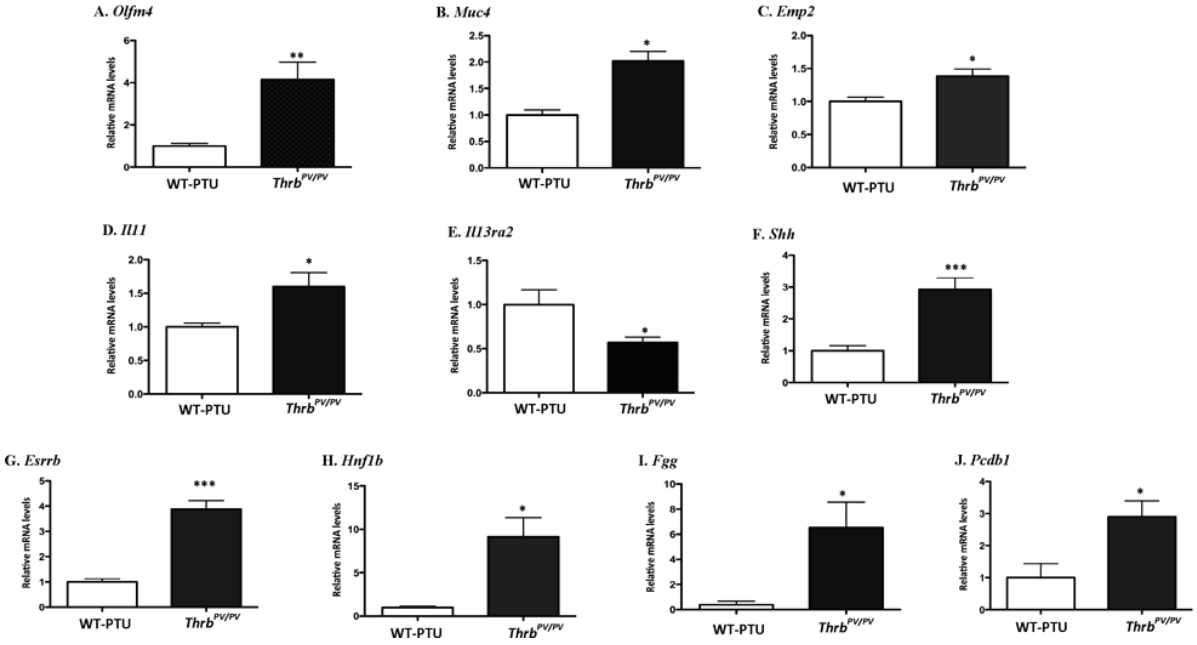

Figure 2. Validation of microarray results by real time RT-PCR. Total RNA was extracted from thyroids of *Thrb*$^{PV/PV}$ and WT-PTU mice at the age of 10-12 months, and real time RT-PCR was performed as described in Materials and methods. Fold of changes of the expression of mRNA is shown. An "*" indicates $p<0.05$, "**" represents $p<0.01$, and "***" represents $p<0.001$ by the Student's *t* test. Gene being validated is indicated in each figure (A-J).

adhesion and invasion revealed that an array of genes shown in **Table 1** participated in complex signaling to mediate metastatic thyroid carcinogenesis of *Thrb*$^{PV/PV}$ mice.

Identification of critical tumor-related genes in thyroid tumor cells of Thrb$^{PV/PV}$ *mice*

In addition to the metastasis-related genes (**Table 1**), we identified 35 genes (23.3%; 35/150 total genes) involved in tumor development in the microdissected thyroid lesions of *Thrb*$^{PV/PV}$ mice (**Table 2**). About 65.7% of genes in this group were activated, with changes ranging from 1.53- to 10.9-fold; 34.2% were repressed, with changes ranging from 1.49- to 10-fold. These genes are key regulators in embryonic development, differentiation, transcription regulation, and signaling transduction. The altered expression of these genes suggested that they are critical in the oncogenesis of thyroid tumor cells. Of particular interest was the activated expression of the sonic hedgehog homolog (*Shh*) gene (5.8-fold; **Table 2**) that was further confirmed by real time RT-PCR analysis (**Figure 2F**). Shh is a secreted protein that plays a key role in embryogenesis and thyroid morphogenesis [27]. Importantly, it controls cell division of adult stem cells and has been implicated in the development of several cancers by promoting angiogenesis or cancer stem cell renewal [28, 29].

Another gene that plays a pivotal role in tissue regeneration and cancer development is the estrogen-related receptor β (*Esrrb*) gene that encodes an orphan nuclear receptor, Esrrβ (Nr3b2). Consistent with the array data (4-fold up-regulated; **Table 2**), real time RT-PCR analysis showed that the mRNA expression of *Esrrb* was increased nearly 3-fold (**Figure 2G**). In conjunction with other transcription factors critical for pluripotency of stem cells, namely Oct4 and Sox2, Esrrβ could also act to induce fibroblasts into pluripotent stem cells by targeting genes involved in self-renewal and pluripotency [30]. The findings that *Shh* and *Esrrb* were activated in the thyroid lesions of *Thrb*$^{PV/PV}$ mice raised the possibility that adult cancer stem cells could be involved in the oncogenesis of thyroid cancer.

Table 2 shows the activation of another oncogene, the hepatocyte nuclear factor 1b gene (*Hnf1b*) (1.95-fold; Table 2). A 6.0-fold increase in mRNA expression was detected by real time RT-PCR (Figure 2H). The *Hnf1b* gene encodes a homeobox transcription factor that was recently found aberrantly expressed in several human neoplasms, such as ovarian clear cell carcinoma, and thyroid cancer [31, 32]. In thyroid cancers, *HNF1b* mRNA and protein were detected in several papillary cancer cell lines containing RET-PTC1 translocation. Its high expression (Figure 2H) suggested its pivotal role in the metastatic thyroid carcinogenesis of $Thrb^{PV/PV}$ mice.

The 10.9-fold activated expression of the fibrinogen gamma chain (*Fgg*) gene was highly relevant in the understanding of the metastatic process of thyroid cancer (see also Figure 2I). This gene encodes a subunit (gamma-fibrinogen) of fibrinogen that is associated with human cancers such as hepatocarcinoma [33]. Importantly, fibrinogen is known to function as a ligand to activate integrins α5β1 and αvβ3 signaling to affect downstream signaling to increase cell motility and invasion. Indeed, our recent findings showed that an activated integrin signaling promotes thyroid carcinogenesis of $Thrb^{PV/PV}$ mice [13].

Altered expression of genes with diverse cellular functions in thyroid tumor cells of $Thrb^{PV/PV}$ mice

Analyses of the array data further showed altered expression of 56 genes important in various cellular processes (Table 3). These genes represent 37.3% of total genes identified. Among these genes, 31 were up-regulated and 25 were down-regulated. Twenty-three of them (41%) were regulators with enzymatic activity related to metabolic synthesis, protein/lipid phosphorylation, protein degradation, or DNA modification. Six genes (10.7%) had biological activities related to intracellular trafficking, and there were transporter-related genes. The remaining 24 genes were associated with transcriptional regulation or post-transcriptional modification or served as membrane receptors in mediating cell-cell or cell-extracellular matrix (ECM) interaction. Thus, the metastatic process of thyroid tumor cells requires not only that genes function directly in mediating cell invasion and migration, but also that genes actively participate in a variety of cellular functions. Indeed, it is known that transformation of cells from a normal to a cancerous state is usually accompanied by reprogramming of metabolic pathways, including those that regulate glycolysis and the production of lipids. The altered gene repertoire of metastasis-related genes in $Thrb^{PV/PV}$ thyroids thus extends to metabolism-related enzymes, such as carbonic anhydrase IV (*Ca4*) in carbon dioxide hydration, glutamic-oxaloacetic transaminase 1 (*Got1*) in amino acid metabolism, and pterin-4-a-carbinolamine dehydratase (*Pcbd1*; Figure 2J) in phenylalanine hydroxylation (Table 3).

In addition to genes related to metabolic enzymes, we also found a set of genes related to intracellular trafficking and transport. Two large families of molecular motors—kinesins and dyneins—drive transport along microtubule filaments. Many molecules are translocated in and out of different cellular compartments via this system, for example, p53, glucocorticoid receptors, and androgen receptors. Two members of molecular motor families, kinesin family member 5C (*Kif5c*) and dynein cytoplasmic intermediate chain 1 (*Dync1i1*), were found to be up-regulated in $Thrb^{PV/PV}$ thyroid (Table 3). Several genes involved in vesicle-mediated transport were also preferentially expressed in $Thrb^{PV/PV}$ thyroids, such as golgi-specific brefeldin A resistant guanine nucleotide exchange factor 1 (*Gbf1*), TBC1 domain family member 20 (*Tbc1d20*), and Golgi integral membrane protein 4 (*Golim4*). These changes in the expression may affect re-localization of certain molecules to indirectly regulate their functions.

The final group of genes that encode enzymatic proteins revealed in the present study is ubiquitination system-related genes. The ubiquitin–proteasome pathway is critical in the degradation of a majority of cellular proteins. Increased deubiquitinating (DUB) enzymes may not only enhance the protein stability, but also affect several biochemical pathways relevant to cancers, such as internalization and degradation of receptor tyrosine kinases, transcription regulation, activation or localization of signaling intermediates, and cell cycle progression [34]. The present array analysis showed one up-regulated DUB enzyme gene (ubiquitin specific peptidase 3, *Usp3*) and three down-regulated DUBs (OUT domain containing 7A, *Otud7a*; ubiquitin specific peptidase 37, *Usp37*; zinc finger, RNA-binding domain containing1, *Zranb1*) in thyroid

tumors of *Thrb*$^{PV/PV}$ mice (**Table 3**). Among these DUBs, USP3 has been shown to efficiently deubiquitinate histone H2A and H2B. Its depletion can lead to the arrest of the cell cycle in the S-phase [35]. On the basis of these important cellular functions, it is reasonable to propose that they function to facilitate the metastatic process of thyroid tumor cells of *Thrb*$^{PV/PV}$ mice.

Discussion

Extensive molecular analyses have clearly shown that the *Thrb*$^{PV/PV}$ mouse is a valid mouse model for dissecting changes in molecular genetics underlying follicular thyroid carcinogenesis. Our recent studies further demonstrated that TSH is necessary for the proliferation of thyrocytes, but not sufficient to drive the metastasis of hyperplastic thyrocytes. The mutant TRβPV is required to empower the hyperplastic thyrocytes to invade and to metastasize to distant sites [13]. This observation has facilitated our genomic profiling of genes contributing to metastatic carcinogenesis of *Thrb*$^{PV/PV}$ mice. We first compared the gene expression patterns between WT and WT-PTU to identify altered gene expression due to the growth stimulatory effect of TSH. As *Thrb*$^{PV/PV}$ mice exhibit highly elevated TSH, the comparison of gene expression patterns between WT and *Thrb*$^{PV/PV}$ mice yielded altered expression of genes due to the combined effects of TSH and TRβPV. By further comparison between TSH-mediated effects (WT-PTU mice) and combined TSH- and TRβPV-mediated effects (*Thrb*$^{PV/PV}$ mice), we identified the changes in gene expression that mainly reflected the oncogenic actions of TRβPV in promoting the metastatic process. It is clear from the heat map shown in **Figure 1B** that the gene expression profiles mediated by TSH actions are clearly distinct from those mediated by TRβPV. Therefore, the genes affected by TSH differ from those affected by TRβPV, leading to different pathological consequences. The distinct global changes in gene expression demonstrated in the present study further support our previous conclusions in that without the collaboration of the oncogenic actions of TRβPV, TSH alone is not sufficient to induce metastatic thyroid cancer [13].

By comparing the gene expression profiles of microdissected thyroid cells between WT-PTU and *Thrb*$^{PV/PV}$ mice, we identified genes that contribute to metastatic thyroid carcinogenesis. A total of 150 genes with distinct expression in the tumor cells of *Thrb*$^{PV/PV}$ mice were identified. Clustering of the 87 up-regulated and 63 down-regulated genes with known functions showed that 36% of the genes undergoing changes in expression were related to metastasis and carcinogenesis (see **Table**s **1** & **2**). The remaining genes with known functions (about 37.3% of the total) were involved in various cellular processes including metabolism, intracellular trafficking, transcriptional regulation, post-transcriptional modification, and cell-cell/ECM signaling (**Table 3**). These results clearly indicate that an alteration in global genomic expression is associated with metastatic thyroid cancer. These data further suggest that genes destined to drive the eventual metastasis are present in the primary thyroid lesions.

On the basis of the gene expression profiles and functional clustering, we discerned changes in several signaling networks during metastasis of thyroid tumor cells of *Thrb*$^{PV/PV}$ mice. The enhancement and activation of integrin-ECM signaling was evidenced by increased expression of the *Fgg* and *Emp2* genes, which is consistent with the elevated integrin-c-Src-Fak activity reported previously in *Thrb*$^{PV/PV}$ mice [13]. In addition, Mia1, a negative regulator of integrin-MAPK signaling, was found down-regulated concurrently with an increased expression of its negative regulator, Hmga1. Adhesion of tumor cells to ECM is a crucial step in the development of cancerous cell metastasis. In human differentiated or anaplastic thyroid carcinoma cells, different patterns of integrin receptors were identified. In follicular thyroid cancer cell lines, high levels of integrins α2, α3, α5, β1, and β3 and low levels of α1 were found, whereas in papillary thyroid cancer cell lines, a dominant expression of integrins a5 and β1 was identified. In undifferentiated anaplastic thyroid cancer cells, integrins α2, α3, α5, α6, and β1 and low levels of α1, α4, and αV were mainly displayed [36]. Taken together, these findings make it clear that the alteration in integrin-ECM signaling plays a crucial role in increasing thyroid tumor cell invasiveness and in promoting distant metastasis in *Thrb*$^{PV/PV}$ mice.

It is important to point out that several key molecules, such as Shh, Esrrb, Nr2f2, and Hnf1b, critical in embryonic development were aberrantly activated in thyroid tumor cells of *Thrb*$^{PV/PV}$ mice. These genes encode transcrip-

tion factors (Esrrb, Nr2f2, and Hnf1b) or signaling regulator (Shh) whose alteration may influence a set of genes related to cell renewal, differentiation, or proliferation. For example, Esrrb can directly activate Oct4 gene expression to maintain cell pluripotency and self-renewal capability [37]. The discovery that these genes are activated in thyroid cancer cells of *Thrb*$^{PV/PV}$ mice raises the possibility that cancer-initiating stem cells could play a role in metastatic thyroid carcinogenesis and that their precise functions warrant additional studies.

These different signaling pathways identified in the present study may coordinate with each other to converge into a larger signaling network to affect the metastatic progression of thyroid cancer cells in *Thrb*$^{PV/PV}$ mice. Three top networks with the highest scores and the greatest number of involved molecules were suggested by analyses of the complete list of genes with altered expression (see Supplemental Table 2). Twenty-five key regulators identified in our array analysis were merged into a network to function mainly in cell death, gene regulation, and cell-to-cell signaling and interaction. In this network, genes related to carcinogenesis, immune responses, and other functions are linked via several important pathways including AKT, NFkB, TGF-β, VEGF, and IFNα signaling. In other two networks, amino acid metabolism can be related to post-translational modification while the post-translational modification is affected by the DNA repair process. These networks could each function individually and/or in a coordinated fashion to bring out the full spectrum of metastatic progression in *Thrb*$^{PV/PV}$ mice.

The present study clearly shows that many aspects of key cellular functions of thyroid tumor cells underwent changes during metastatic processes. That complex alterations of multiple pathways mediate the metastatic process would suggest therapeutic treatments via targeting one single gene or one isolated pathway may not be adequate to ensure total efficacy. However, the key regulators and signaling pathways uncovered in the present study could be studied further to understand molecular mechanisms in the metastatic progression of thyroid cancer. By doing so, it would be possible to understand how best to prevent and/or treat metastasis by using treatment strategies that affect multi-signaling pathways with coordinated molecular targets.

Acknowledgments

This research was supported by the Intramural Research Program of the Center for Cancer Research, National Cancer Institute, NIH. We thank Drs. Xiaolin Wu for assistance in the hybridization of the arrays and preliminary analysis of the data, Jaime Rodriguez-Canales and Jeffrey Hanson, for assistance with the laser capture microdissection experiments.

Please address correspondence to: Sheue-yann Cheng, PhD, Laboratory of Molecular Biology, National Cancer Institute, 37 Convent Dr, Room 5128, Bethesda, MD 20892-4264, USA. Tel: (301) 496-4280; Fax: (301) 402-1344; E-mail: chengs@mail.nih.gov

References

[1] Gillenwater AM and Weber RS. Thyroid carcinoma. Cancer Treat Res 1997; 90: 149-169.
[2] Kaneshige M, Kaneshige K, Zhu X, Dace A, Garrett L, Carter TA, Kazlauskaite R, Pankratz DG, Wynshaw-Boris A, Refetoff S, Weintraub B, Willingham MC, Barlow C and Cheng S. Mice with a targeted mutation in the thyroid hormone beta receptor gene exhibit impaired growth and resistance to thyroid hormone. Proc Natl Acad Sci U S A 2000; 97: 13209-13214.
[3] Parrilla R, Mixson AJ, McPherson JA, McClaskey JH and Weintraub BD. Characterization of seven novel mutations of the c-erbA beta gene in unrelated kindreds with generalized thyroid hormone resistance. Evidence for two "hot spot" regions of the ligand binding domain. The Journal of Clinical Investigation 1991; 88: 2123-2130.
[4] Ono S, Schwartz ID, Mueller OT, Root AW, Usala SJ and Bercu BB. Homozygosity for a dominant negative thyroid hormone receptor gene responsible for generalized resistance to thyroid hormone. J Clin Endocrinol Metab 1991; 73: 990-994.
[5] Suzuki H, Willingham MC and Cheng SY. Mice with a mutation in the thyroid hormone receptor beta gene spontaneously develop thyroid carcinoma: a mouse model of thyroid carcinogenesis. Thyroid 2002; 12: 963-969.
[6] Furuya F, Hanover JA and Cheng SY. Activation of phosphatidylinositol 3-kinase signaling by a mutant thyroid hormone beta receptor. Proc Natl Acad Sci U S A 2006; 103: 1780-1785.
[7] Ringel MD, Hayre N, Saito J, Saunier B, Schuppert F, Burch H, Bernet V, Burman KD, Kohn LD and Saji M. Overexpression and overactivation of Akt in thyroid carcinoma. Cancer Res 2001; 61: 6105-6111.
[8] Ying H, Suzuki H, Zhao L, Willingham MC, Meltzer P and Cheng SY. Mutant thyroid hormone receptor beta represses the expression and tran-

scriptional activity of peroxisome proliferator-activated receptor gamma during thyroid carcinogenesis. Cancer Res 2003; 63: 5274-5280.
[9] Kato Y, Ying H, Zhao L, Furuya F, Araki O, Willingham MC and Cheng SY. PPARgamma insufficiency promotes follicular thyroid carcinogenesis via activation of the nuclear factor-kappaB signaling pathway. Oncogene 2006; 25: 2736-2747.
[10] Ying H, Furuya F, Zhao L, Araki O, West BL, Hanover JA, Willingham MC and Cheng SY. Aberrant accumulation of PTTG1 induced by a mutated thyroid hormone beta receptor inhibits mitotic progression. J Clin Invest 2006; 116: 2972-2984.
[11] Kim CS, Ying H, Willingham MC and Cheng SY. The pituitary tumor-transforming gene promotes angiogenesis in a mouse model of follicular thyroid cancer. Carcinogenesis 2007; 28: 932-939.
[12] Guigon CJ, Zhao L, Lu C, Willingham MC and Cheng SY. Regulation of beta-catenin by a novel nongenomic action of thyroid hormone beta receptor. Mol Cell Biol 2008; 28: 4598-4608.
[13] Lu C, Zhao L, Ying H, Willingham MC and Cheng SY. Growth activation alone is not sufficient to cause metastatic thyroid cancer in a mouse model of follicular thyroid carcinoma. Endocrinology 2010; 151: 1929-1939.
[14] Dennis G, Jr., Sherman BT, Hosack DA, Yang J, Gao W, Lane HC and Lempicki RA. DAVID: Database for Annotation, Visualization, and Integrated Discovery. Genome Biol 2003; 4: P3.
[15] Huang da W, Sherman BT and Lempicki RA. Systematic and integrative analysis of large gene lists using DAVID bioinformatics resources. Nat Protoc 2009; 4: 44-57.
[16] Fontaine JF, Mirebeau-Prunier D, Raharijaona M, Franc B, Triau S, Rodien P, Goeau-Brissonniere O, Karayan-Tapon L, Mello M, Houlgatte R, Malthiery Y and Savagner F. Increasing the number of thyroid lesions classes in microarray analysis improves the relevance of diagnostic markers. PLoS One 2009; 4: e7632.
[17] Yasui W, Oue N, Aung PP, Matsumura S, Shutoh M and Nakayama H. Molecular-pathological prognostic factors of gastric cancer: a review. Gastric Cancer 2005; 8: 86-94.
[18] Grutzmann R, Pilarsky C, Staub E, Schmitt AO, Foerder M, Specht T, Hinzmann B, Dahl E, Alldinger I, Rosenthal A, Ockert D and Saeger HD. Systematic isolation of genes differentially expressed in normal and cancerous tissue of the pancreas. Pancreatology 2003; 3: 169-178.
[19] Li SR, Dorudi S and Bustin SA. Identification of differentially expressed genes associated with colorectal cancer liver metastasis. Eur Surg Res 2003; 35: 327-336.
[20] Buisine MP, Desreumaux P, Leteurtre E, Copin MC, Colombel JF, Porchet N and Aubert JP. Mucin gene expression in intestinal epithelial cells in Crohn's disease. Gut 2001; 49: 544-551.
[21] Copin MC, Buisine MP, Leteurtre E, Marquette CH, Porte H, Aubert JP, Gosselin B and Porchet N. Mucinous bronchioloalveolar carcinomas display a specific pattern of mucin gene expression among primary lung adenocarcinomas. Hum Pathol 2001; 32: 274-281.
[22] Wadehra M, Forbes A, Pushkarna N, Goodglick L, Gordon LK, Williams CJ and Braun J. Epithelial membrane protein-2 regulates surface expression of alphavbeta3 integrin in the endometrium. Dev Biol 2005; 287: 336-345.
[23] Sales KJ, Grant V, Cook IH, Maldonado-Perez D, Anderson RA, Williams AR and Jabbour HN. Interleukin-11 in endometrial adenocarcinoma is regulated by prostaglandin F2alpha-F-prostanoid receptor interaction via the calcium-calcineurin-nuclear factor of activated T cells pathway and negatively regulated by the regulator of calcineurin-1. Am J Pathol 176: 435-445.
[24] Yoshizaki A, Nakayama T, Yamazumi K, Yakata Y, Taba M and Sekine I. Expression of interleukin (IL)-11 and IL-11 receptor in human colorectal adenocarcinoma: IL-11 up-regulation of the invasive and proliferative activity of human colorectal carcinoma cells. Int J Oncol 2006; 29: 869-876.
[25] Shimamura T, Fujisawa T, Husain SR, Joshi B and Puri RK. Interleukin 13 mediates signal transduction through interleukin 13 receptor alpha2 in pancreatic ductal adenocarcinoma: role of IL-13 Pseudomonas exotoxin in pancreatic cancer therapy. Clin Cancer Res 2010; 16: 577-586.
[26] Yan X, Su Z, Zhang J, Wu Z, Ye S, Lu X, Wu J, Zeng Y and Zheng W. Killing effect of interleukin-13 receptor alpha 2 (IL-13R[alpha]2) sensitized DC-CTL cells on human glioblastoma U251 cells. Cellular Immunology In Press, Corrected Proof:
[27] Fagman H, Grande M, Gritli-Linde A and Nilsson M. Genetic deletion of sonic hedgehog causes hemiagenesis and ectopic development of the thyroid in mouse. Am J Pathol 2004; 164: 1865-1872.
[28] Kanda S, Mochizuki Y, Suematsu T, Miyata Y, Nomata K and Kanetake H. Sonic hedgehog induces capillary morphogenesis by endothelial cells through phosphoinositide 3-kinase. J Biol Chem 2003; 278: 8244-8249.
[29] Li C, Heidt DG, Dalerba P, Burant CF, Zhang L, Adsay V, Wicha M, Clarke MF and Simeone DM. Identification of pancreatic cancer stem cells. Cancer Res 2007; 67: 1030-1037.
[30] Feng B, Jiang J, Kraus P, Ng JH, Heng JC, Chan YS, Yaw LP, Zhang W, Loh YH, Han J, Vega VB, Cacheux-Rataboul V, Lim B, Lufkin T and Ng HH. Reprogramming of fibroblasts into induced pluripotent stem cells with orphan nuclear receptor Esrrb. Nat Cell Biol 2009; 11: 197-203.
[31] Tsuchiya A, Sakamoto M, Yasuda J, Chuma M, Ohta T, Ohki M, Yasugi T, Taketani Y and Hirohashi S. Expression Profiling in Ovarian Clear Cell Carcinoma: Identification of Hepatocyte Nuclear

Factor-1{beta} as a Molecular Marker and a Possible Molecular Target for Therapy of Ovarian Clear Cell Carcinoma. Am J Pathol 2003; 163: 2503-2512.
[32] Xu J, Capezzone M, Xu X and Hershman JM. Activation of nicotinamide N-methyltransferase gene promoter by hepatocyte nuclear factor-1beta in human papillary thyroid cancer cells. Mol Endocrinol 2005; 19: 527-539.
[33] Zhu WL, Fan BL, Liu DL and Zhu WX. Abnormal expression of fibrinogen gamma (FGG) and plasma level of fibrinogen in patients with hepatocellular carcinoma. Anticancer Res 2009; 29: 2531-2534.
[34] Singhal S, Taylor M and Baker R. Deubiquitylating enzymes and disease. BMC Biochemistry 2008; 9: S3.
[35] Nicassio F, Corrado N, Vissers JH, Areces LB, Bergink S, Marteijn JA, Geverts B, Houtsmuller AB, Vermeulen W, Di Fiore PP and Citterio E. Human USP3 is a chromatin modifier required for S phase progression and genome stability. Curr Biol 2007; 17: 1972-1977.
[36] Hoffmann S, Maschuw K, Hassan I, Reckzeh B, Wunderlich A, Lingelbach S and Zielke A. Differential pattern of integrin receptor expression in differentiated and anaplastic thyroid cancer cell lines. Thyroid 2005; 15: 1011-1020.
[37] Zhang X, Zhang J, Wang T, Esteban MA and Pei D. Esrrb activates Oct4 transcription and sustains self-renewal and pluripotency in embryonic stem cells. J Biol Chem 2008; 283: 35825-35833.
[38] Benjamini Y and Hochberg Y. Controlling the false discovery rate: a practical and powerful approach to multiple testing. J. Roy. Statist. Soc. Ser. B 1995; 57: 289–300.

Supplementary Table 1. Primer sequences used for determination of gene expression by real time RT-PCR

	Name	Primer sequence	Amplicon size (bps)
1	mCldn6-F1-85	5'-agacaaagctgaccgagcac-3'	213
	mCldn6-R1-297	5'-gctctgaaccacacaggaca-3'	
2	mCxcl17-F1-135	5'-tgttgcttccagtgatgctc-3'	169
	mCxcl17-R1-303	5'-gctgtggctttttctctttgg-3'	
3	mDdr1-F2-856	5'-gggcagaccatgcagttatc-3'	187
	mDdr1-R2-1042	5'-tgctccatcccacatagtca-3'	
4	mEmp2-F1-354	5'-ctctggagagtgtgcaccaa-3'	198
	mEmp2-R1-551	5'-cgtcaggacgaacctctctc-3'	
5	mEsrrb-F1-809	5'-ggcgttcttcaagagaacca-3'	225
	mEsrrb-R1-1033	5'-aggttcaggtaggggctgtt-3'	
6	mFgg-F1-1030	5'-tgggacaacgacaacgataa-3'	155
	mFgg-R1-1184	5'-ccgtcgtcgaaaccattagt-3'	
7	mGAPDH-R2-674	5'-ggatgcagggatgatgttct-3'	239
	mGAPDH-F2-436	5'-ttgtgatgggtgtgaaccac-3'	
8	mGrhl2-F1-1858	5'-tgccagtggagaaaatcaca-3'	155
	mGrhl2-R1-2010	5'-ctccatcagcgtgatcttga-3'	
9	mGrhl3-F1-1529	5'-acatacttgcggccagaaac-3'	174
	mGrhl3-R1-1702	5'-aggctcaaactcctcagcaa-3'	
10	mHnf1b-F2-1201	5'-ctcctctccacccaacaaga-3'	203
	mHnf1b-R2-1403	5'-ccgacactgtgatctgcatt-3'	
11	mIl11-F1-400	5'-ctgggacattgggatctttg-3'	236
	mIl11-R1-635	5'-ggggatcacaggttggtct-3'	
12	mIL13ra2-F2-548	5'-cgcatttgtcagagcattgt-3'	218
	mIL13ra2-R2-765	5'-atccaagccctcataccaga-3'	
13	mLad1-F1-1737	5'-gcgacacctctttgagaagg-3'	187
	mLad1-R1-1923	5'-agccctcttggtgactgatg-3'	
14	mMia1-F1-272	5'-tgattgccgcttcttgacta-3'	155
	mMia1-R1-426	5'-ggacaatgctactggggaaa-3'	
15	mMuc4-F2-8879	5'-ctttgcggctcaatacaaca-3'	176
	mMuc4-R2-9054	5'-cattttgggtcagcagaaca-3'	
16	mNr2f2-F1-566	5'-tttcacccgccaaactaaag-3'	181
	mNr2f2-R1-746	5'-caggtacgagtggcagttga-3'	
17	mOlfm4-F2-241	5'-ggacctgccagtgttctgtt-3'	188
	mOlfm4-R2-428	5'-gacctctactcggaccgtca-3'	
18	mPcbd1-F1-158	5'-aggccgagatgctatcttca-3'	161
	mPcbd1-R1-318	5'-cacattcatgggtgctcaag-3'	
19	mRfx4-F1-1639	5'-gaccgatgcgttgtaaaggt-3'	180
	mRfx4-R1-1818	5'-gagcacgtagtcgtcgaaca-3'	
20	mSlc39a4-F1-458	5'-gacgattacctggccacact-3'	226
	mSlc39a4-R1-683	5'-cttggaagcaggacccatta-3'	
21	mShh-F1-533	5'-gaagatcacaagaaactccgaacg-3'	170
	mShh-R1-702	5'-cactccaggccactggttc-3'	

Supplementary Table 2. Complete list of genes with altered expression (n=150) in thyroid tumors of *Thrb*$^{PV/PV}$

Gene symbol	Accession no.	Adjusted P value	Fold change	Gene name
Upregulated genes				
Fgg	NM_133862	0.025	10.868	fibrinogen gamma chain
Slc39a4	BC023498	0.034	9.088	solute carrier family 39 (zinc transporter), member 4
Car4	NM_007607	0.025	6.695	carbonic anhydrase 4
Slc5a5	AF380353	0.024	5.979	solute carrier family 5 (sodium iodide symporter), member 5
Shh	AV304616	0	5.804	sonic hedgehog
Got1	AA792094	0.037	5.784	glutamate oxaloacetate transaminase 1, soluble
Fam163a	BB183509	0.005	5.626	family with sequence similarity 163, member A
Olfm4	AV290148	0.025	5.517	olfactomedin 4
Bcat1	X17502	0.035	5.22	branched chain aminotransferase 1, cytosolic
Gm266	BB829749	0.008	5.032	predicted gene 266
Ppp2r3a	AI642021	0.016	4.636	protein phosphatase 2 (formerly 2A), regulatory subunit B", alpha
Sbf1	AV121839	0.035	4.389	SET binding factor 1
Esrrb	AV333667	0.024	4.003	estrogen related receptor, beta
Muc4	AF218265	0.033	3.853	mucin 4
B4galnt2	AI593864	0.017	3.548	beta-1,4-N-acetyl-galactosaminyl transferase 2
8430419L09Rik	NM_028982	0.022	3.541	RIKEN cDNA 8430419L09 gene
Lad1	NM_133664	0.024	3.354	ladinin
Slc22a23	BM234253	0.019	3.278	solute carrier family 22, member 23
Ankrd40	BB213578	0.016	3.229	ankyrin repeat domain 40
Cldn6	BC005718	0.03	3.215	claudin 6
Fxyd4	NM_033648	0.025	3.112	FXYD domain-containing ion transport regulator 4
Tmed6	NM_025458	0.013	2.969	transmembrane emp24 protein transport domain containing 6
Kif5c	AI844677	0.039	2.936	kinesin family member 5C
Rbm20	AK003783	0.024	2.906	RNA binding motif protein 20
Kdm6b	BB494168	0.03	2.876	KDM1 lysine (K)-specific demethylase 6B
Pcbd1	NM_025273	0.015	2.864	pterin 4 alpha carbinolamine dehydratase/dimerization cofactor of hepatocyte nuclear factor 1 alpha (TCF1) 1
BC017612	NM_133214	0.045	2.848	cDNA sequence BC017612
AI314604	BE991175	0.016	2.819	expressed sequence AI314604
C4bp	NM_007576	0.01	2.815	complement component 4 binding protein
Dusp14	AK009744	0.034	2.793	dual specificity phosphatase 14
Suclg2	BF608645	0.017	2.778	succinate-Coenzyme A ligase, GDP-forming, beta subunit
Slmo1	BB835597	0.017	2.766	slowmo homolog 1 (Drosophila)
Mtm1	NM_019926	0.039	2.732	X-linked myotubular myopathy gene 1
B3gnt1	AV032053	0.043	2.654	UDP-GlcNAc:betaGal beta-1,3-N-acetylglucosaminyltransferase 1
Tceal1	BC011290	0.037	2.65	transcription elongation factor A (SII)-like 1
Rshl2a	AA544511	0.037	2.643	radial spokehead-like 2A; radial spoke 3A homolog (Chlamydomonas)
Mapk6	BC024684	0.033	2.588	mitogen-activated protein kinase 6 (Extracellular signal-regulated kinase 3) (ERK-3)
Thy1	AV028402	0.03	2.574	thymus cell antigen 1, theta
Grhl3	AV231424	0.013	2.53	grainyhead-like 3 (Drosophila)
Trpm3	BB125842	0.037	2.53	transient receptor potential cation channel, subfamily M, member 3
Ddr1	BF225985	0.049	2.497	discoidin domain receptor family, member 1
Rcor1	AW543416	0.028	2.493	REST corepressor 1
LOC100045988	BM199323	0.039	2.49	similar to OPR
Socs1	AB000710	0.015	2.474	suppressor of cytokine signaling 1
Lsm2	AF204156	0.025	2.466	LSM2 homolog, U6 small nuclear RNA associated (S. cerevisiae)
Emp2	AF083876	0.032	2.427	epithelial membrane protein 2
Gm941	BB479096	0.032	2.4	predicted gene 941
Dync1i1	NM_010063	0.046	2.351	dynein cytoplasmic 1 intermediate chain 1
Fut9	AU067636	0.013	2.317	fucosyltransferase 9
Rtn4ip1	NM_130892	0.01	2.299	reticulon 4 interacting protein 1
Lamc2	NM_008485	0.018	2.259	laminin, gamma 2
Rfx4	AV255458	0.024	2.253	regulatory factor X, 4 (influences HLA class II expression)
Mt3	NM_013603	0.022	2.208	metallothionein 3

Atrn	AW558010	0.043	2.181	attractin
Grhl2	AK005410	0.049	2.099	grainyhead-like 2 (Drosophila)
Rnasek	BI156989	0.047	2.094	ribonuclease, RNase K
Psd3	NM_030263	0.027	2.088	pleckstrin and Sec7 domain containing 3
Lonp1	AK004820	0.026	2.083	lon peptidase 1, mitochondrial
Rfx5	BB392192	0.013	2.076	regulatory factor X, 5 (influences HLA class II expression)
A330068G13Rik	BB246530	0.045	2.062	RIKEN cDNA A330068G13 gene
3110043021Rik	AK014175	0.034	2.02	RIKEN cDNA 3110043021 gene
Map6d1	BB762333	0.045	1.951	MAP6 domain containing 1
Hnf1b	AI987804	0.024	1.949	HNF1 homeobox B
Hira	AW537496	0.017	1.94	histone cell cycle regulation defective homolog A (S. cerevisiae)
C030005G22Rik	BB355326	0.024	1.935	RIKEN cDNA C030005G22 gene
Gfra1	BE534815	0.025	1.904	glial cell line derived neurotrophic factor family receptor alpha 1
Ppif	NM_134084	0.043	1.883	peptidylprolyl isomerase F (cyclophilin F)
Arl13b	AV225959	0.017	1.856	ADP-ribosylation factor-like 13B
2210409E12Rik	NM_028218	0.008	1.835	RIKEN cDNA 2210409E12 gene; coilin
Hmga1	NM_016660	0.048	1.826	high mobility group AT-hook I, related sequence 1
Rrn3	AA866997	0.028	1.815	RRN3 RNA polymerase I transcription factor homolog (yeast)
Idh2	NM_008322	0.032	1.81	isocitrate dehydrogenase 2 (NADP+), mitochondrial
Ccnj	BB051001	0.024	1.764	cyclin J
Med20	NM_020048	0.032	1.759	mediator complex subunit 20
Fastkd3	AK009264	0.043	1.739	FAST kinase domains 3
4930420K17Rik	BB323696	0.024	1.727	RIKEN cDNA 4930420K17 gene
Cyb5b	NM_025558	0.024	1.697	cytochrome b5 type B
BC037704	BM938208	0.045	1.691	cDNA sequence BC037704
Tomm40	AF109918	0.033	1.654	translocase of outer mitochondrial membrane 40 homolog (yeast)
Egln3	BB284358	0.043	1.646	EGL nine homolog 3 (C. elegans)
Flrt1	BQ173985	0.03	1.638	fibronectin leucine rich transmembrane protein 1
Il11	NM_008350	0.028	1.637	interleukin 11
Usp3	BM206593	0.04	1.56	ubiquitin specific peptidase 3
Hspa4l	NM_011020	0.048	1.535	heat shock protein 4 like
Lrrc47	AK013512	0.016	1.523	leucine rich repeat containing 47
Dph2	AK011199	0.024	1.51	DPH2 homolog (S. cerevisiae)
Gbf1	BM948896	0.013	1.506	golgi-specific brefeldin A-resistance factor 1
Downregulated genes				
Krt8	M21836	0.05	0.667	keratin 8
Otud7a	NM_130880	0.043	0.647	OTU domain containing 7A
Rnf130	BE948550	0.037	0.644	ring finger protein 130
BC063263	BM211194	0.048	0.625	cDNA sequence BC063263
Ttc13	BB492914	0.043	0.605	tetratricopeptide repeat domain 13
Sp3	AK004607	0.044	0.602	trans-acting transcription factor 3
C430049A07Rik	AK021261	0.015	0.595	RIKEN cDNA C430049A07 gene
Rpl11	AK014593	0.009	0.594	ribosomal protein L11
2900010M23Rik	AV046927	0.024	0.584	RIKEN cDNA 2900010M23 gene
N6amt2	BF730076	0.049	0.584	N-6 adenine-specific DNA methyltransferase 2 (putative)
Sra1	BG074964	0.028	0.576	steroid receptor RNA activator 1
Gfod1	AV220135	0.028	0.576	glucose-fructose oxidoreductase domain containing 1
Foxn3	BM196962	0.049	0.572	forkhead box N3
Mbd5	BB086698	0.048	0.57	methyl-CpG binding domain protein 5
2810404F17Rik	AK012982	0.048	0.567	RIKEN cDNA 2810404F17 gene
Pnliprp2	AV060116	0.037	0.563	pancreatic lipase-related protein 2
Samd12	AV347618	0.034	0.548	sterile alpha motif domain containing 12
Tacr3	BB498416	0.048	0.543	tachykinin receptor 3
Rpl37a	AV066985	0.048	0.535	ribosomal protein L37a
Il13ra2	BC003723	0.043	0.533	interleukin 13 receptor, alpha 2
Elf2	BC027739	0.048	0.518	E74-like factor 2
Agr2	AV066597	0.007	0.511	anterior gradient 2 (Xenopus laevis)
Thap4	BB130418	0.024	0.505	THAP domain containing 4
BB187676	BB313560	0.01	0.501	expressed sequence BB187676
Rock1	BI662863	0.024	0.5	Rho-associated coiled-coil containing protein kinase 1
Rnf166	BB870298	0.03	0.5	ring finger protein 166
Trove2	BQ176653	0.043	0.499	TROVE domain family, member 2

Dnm3os	BB542096	0.008	0.491	dynamin 3, opposite strand
Impact	BB524087	0.015	0.481	imprinted and ancient
Oxtr	BB551848	0.044	0.475	oxytocin receptor
Tgs1	BM233196	0.045	0.465	trimethylguanosine synthase homolog (S. cerevisiae)
Usp37	BB398605	0.037	0.461	ubiquitin specific peptidase 37
D1Ertd75e	BG066069	0.016	0.459	DNA segment, Chr 1, ERATO Doi 75, expressed
Tbc1d20	BC002196	0.044	0.452	TBC1 domain family, member 20
Rpl37	BF578245	0.027	0.45	ribosomal protein L37
1700029I01Rik	BQ033755	0.037	0.445	RIKEN cDNA 1700029I01 gene
AI481207	AI481207	0.048	0.439	expressed sequence AI481207
Alcam	AV315205	0.047	0.437	activated leukocyte cell adhesion molecule
Fjx1	AV230815	0.017	0.436	four jointed box 1 (Drosophila)
Spnb2	BM213516	0.044	0.435	spectrin beta 2
Sec14l2	BC005759	0.028	0.426	SEC14-like 2 (S. cerevisiae)
Lman1	BG071597	0.044	0.425	lectin, mannose-binding, 1
Zcchc14	BB223737	0.015	0.413	zinc finger, CCHC domain containing 14
Golim4	BM942873	0.014	0.41	golgi integral membrane protein 4
Fstl1	BI452727	0.037	0.404	follistatin-like 1
Olfm1	BB549310	0.025	0.366	olfactomedin 1
Afp	NM_007423	0.045	0.363	alpha fetoprotein
Taok1	BB151477	0.044	0.349	TAO kinase 1
Tmod3	BB224629	0.017	0.347	tropomodulin 3
Cacna2d1	BB559910	0.03	0.347	calcium channel, voltage-dependent, alpha2/delta subunit 1
Cldnd1	AK012260	0.039	0.347	claudin domain containing 1
Pdlim4	NM_019417	0.005	0.335	PDZ and LIM domain 4
Mia1	NM_019394	0.016	0.332	melanoma inhibitory activity 1
Slc12a2	BG069505	0.024	0.331	solute carrier family 12, member 2
Ggps1	NM_010282	0.045	0.306	geranylgeranyl diphosphate synthase 1
Nr2f2	BB053811	0.044	0.301	nuclear receptor subfamily 2, group F, member 2
Rc3h2	BB527789	0.035	0.299	ring finger and CCCH-type zinc finger domains 2
Atxn2	BE953583	0.009	0.286	ataxin 2
Tor1b	BB004887	0.03	0.276	torsin family 1, member B
Zfp871	BB008634	0.008	0.254	zinc finger protein 871
Cxcl17	BC024561	0.015	0.227	chemokine (C-X-C motif) ligand 17
Map3k2	AV381143	0.028	0.192	mitogen-activated protein kinase kinase kinase 2
Prdm6	AV303905	0.031	0.102	PR domain containing 6

Supplementary Table 3. Functional analysis of genes (n=150) with aberrant expression in thyroid tumors of *Thrb*$^{PV/PV}$ mice

	Sub-Category	p-value	Molecules
Cell development and differentiation	Reproductive System Development and Function	1.36E-04-4.4E-02	MUC4, OXTR, IL11, AFP, HIRA, SLC12A2, KRT8, ESRRB, DDR1, SOCS1, SP3, SHH
	Embryonic Development	6.01E-04-4.4E-02	ARL13B, IL11, HIRA, HNF1B, MAP3K2, KRT8, ESRRB, HMGA1, GRHL3, SHH
	Digestive System Development and Function	1.42E-03-3.78E-02	HNF1B, SLC12A2, GFRA1, SPTBN1, SHH
	Hematological System Development and Function	2.16E-03-4.4E-02	IL11, ROCK1, FGG, MAP3K2, ATRN, DDR1, THY1, SOCS1, HMGA1, SP3, SHH
	Renal and Urological System	6.25E-03-	IL11, HNF1B, GFRA1, THY1, SHH

	Development and Function	4.4E-02	
	Nervous System Development and Function	4.61E-03-4.4E-02	OLFM1, ROCK1, RFX4, ATRN, GFRA1, SHH, KIF5C, MT3, IL11, HNF1B, FUT9, ALCAM, RTN4, THY1, NR2F2
	Connective Tissue Development and Function	6.14E-03-4.4E-02	MIA, IL11, ROCK1, KRT8, RTN4, THY1, SHH
	Endocrine System Development and Function	6.41E-03-4.4E-02	AFP, KRT8, SLC5A5, SOCS1, HMGA1, SHH
	Cardiovascular System Development and Function	6.41E-03-3.78E-02	HNF1B, DDR1, RTN4, IL13RA2, THY1, NR2F2, SHH
Disease-related	Gastrointestinal Disease	2.56E-04-2.54E-02	RFX4, TACR3, ESRRB, IL13RA2, SOCS1, LAMC2, GFRA1, TRPM3, SAMD12, SP3, SHH, GFOD1, USP3, IL11, GOT1, SUCLG2, HIRA, DYNC1I1, KRT8, ALCAM, FOXN3
	Genetic Disorder	1.77E-03-4.4E-02	PSD3, TTC13, ATRN, TRPM3, RRN3, SP3, SLC39A4, SHH, USP3, FSTL1, MT3, SUCLG2, HIRA, ALCAM, FOXN3, RTN4, RFX5, SLC22A23, MATR3, LMAN1, MBD5, RNF130, TACR3, PDLIM4, GFRA1, GOT1, DYNC1I1, FUT9, THY1, B3GNT1, GBF1, DDR1, SAMD12, CA4, PCBD1, ATXN2, HNF1B, FGG, CYB5B, GRHL2, OLFM1, RFX4, SLC12A2, TAOK1, ZRANB1, ESRRB, MTM1, SLC5A5, IL13RA2, SOCS1, LAMC2, GFOD1, TOMM40, KRT8, HMGA1, SPTBN1
	Renal and Urological Disease	1.77E-03-1.91E-02	HNF1B, DDR1, SOCS1
	Endocrine System Disorders	3.04E-03-3.16E-02	PSD3, TTC13, GBF1, DDR1, TRPM3, SAMD12, USP3, CA4, HNF1B, ATXN2, LSM2, GRHL2, ALCAM, FOXN3, TROVE2, RFX4, OTUD7A, PDLIM4, SLC5A5, LAMC2, SOCS1, DYNC1I1, FUT9, THY1, SPTBN1
	Auditory Disease	5.57E-03-1.91E-02	SLC12A2, GRHL2, ESRRB
	Inflammatory Disease	3.65E-03-4.4E-02	PSD3, DDR1, RCOR1, SAMD12, TRPM3, SP3, RRN3, SHH, USP3, CA4, HIRA, SUCLG2, FGG, LSM2, CYB5B, ALCAM, FOXN3, PNLIPRP2, GRHL3, RFX4, ZRANB1, ESRRB, IL13RA2, SOCS1, GFRA1, LAMC2, GOT1, DYNC1I1, GOLIM4
Cell structure and mobility	Cell-To-Cell Signaling and Interaction	1.11E-03-4.4E-02	MUC4, ROCK1, ATRN, DDR1, B4GALNT2, SOCS1, GFRA1, LAMC2, SHH, OXTR, IL11, FGG, KRT8, MAP3K2, ALCAM, THY1
	Tissue Morphology	6.01E-04-4.4E-02	MIA, SLC12A2, ESRRB, DDR1, GFRA1, SOCS1, SHH, KIF5C, IL11, HIRA, HNF1B, KRT8, THY1
	Cell Morphology	1.42E-03-4.4E-02	MIA, TMOD3, ROCK1, GBF1, TAOK1, KRT8, ATRN, RTN4, SOCS1, SHH
	Cellular Movement	4.61E-03-	CXCL17, MIA, ROCK1, DDR1, LAMC2, SOCS1, GFRA1, SHH, FSTL1, KIF5C, IL11, TMOD3,

		4.2E-02	MAP3K2, ALCAM, RTN4, THY1, NR2F2
	Cellular Assembly and Organization	6.41E-03-4.4E-02	MIA, ROCK1, TAOK1, MAP6D1, LAMC2, SOCS1, RRN3, SHH, HNF1B, FGG, KRT8, RTN4, RPL11, SPTBN1
	Tumor Morphology	1.28E-02-2.54E-02	GFRA1, HMGA1, SHH
Immune response	Infection Mechanism	1.11E-03-1.28E-02	IL11, HMGA1
	Cell-mediated Immune Response	2.16E-03-3.16E-02	MAP3K2, SOCS1, HMGA1, SHH
	Hypersensitivity Response	6.41E-03-4.4E-02	IL11, SOCS1
	Inflammatory Response	6.41E-03-3.23E-02	IL11, KRT8, ATRN, DDR1, ALCAM, SOCS1
	Antimicrobial Response	1.28E-02-2.54E-02	MT3, SOCS1
	Immune Cell Trafficking	1.28E-02-2.52E-02	IL11, ROCK1, FGG, MAP3K2, THY1
Cell growth or death	Cellular Growth and Proliferation	2.16E-03-4.4E-02	MUC4, MT3, IL11, SLC12A2, PDLIM4, GFRA1, SOCS1, HMGA1, SHH
	Cell Death	2.74E-03-4.4E-02	PPIF, ROCK1, DDR1, RRN3, SP3, SHH, MT3, FSTL1, IL11, AFP, ATXN2, ALCAM, RTN4, MIA, RPL37, SLC12A2, PDLIM4, SLC5A5, GFRA1, SOCS1, SRA1, KRT8, MAP3K2, EMP2, THY1, HMGA1
	Cell Cycle	6.41E-03-3.16E-02	GFRA1, SOCS1, HMGA1, SHH
	DNA Replication, Recombination, and Repair	6.41E-03-6.41E-03	HIRA, HMGA1
Metabolism-related	Amino Acid Metabolism	1.24E-02-4.03E-02	GOT1, IL11, SBF1, ROCK1, FUT9, MAPK6, TAOK1, MAP3K2, DDR1, B4GALNT2
	Carbohydrate Metabolism	1.28E-02-4.4E-02	MTM1, B4GALNT2, SOCS1
	Lipid Metabolism	1.28E-02-3.78E-02	HNF1B, MTM1, SEC14L2, PNLIPRP2
	Vitamin and	1.28E-	SEC14L2

	Mineral Metabolism Nucleic Acid Metabolism	02- 1.28E- 02 3.16E- 02- 3.16E- 02	 B4GALNT2